Title: A systematic fixed tissue study of the costs and benefits of higher order diffusion models

Elizabeth Hutchinson, Alexandru Avram, Miki Komlosh, Alan Barnett, Evren Ozarslan, Susan Schwerin, Krystaline Radomski, Sharon Juliano and Carlo Pierpaoli

Summary: We have systematically compared four diffusion MRI models – DTI, DKI, MAP-MRI and NODDI – in the same DWI data sets for fixed brain tissue to identify the relative strengths of these approaches and characterize the effects of experimental design and image quality on the generated metrics. Metric-specific advantages in sensitivity and specificity were shown as well as differential vulnerability across the metrics to DWI sampling scheme and noise. The intention of this work is to provide an integrative view of diffusion metrics that contributes to their utility in brain research.

Purpose:
New modeling approaches for diffusion MRI data are promising for improved characterization of non-Gaussian data and the potential for increased sensitivity and specificity. The first goal of this work was to identify and evaluate the benefits of new diffusion MRI frameworks that more fully characterize the diffusion propagator (e.g. DKI and MAP-MRI) or employ biophysical or "microstructure based" modeling (e.g. NODDI). The second goal of this work was to understand the dependence of metrics on the experimental design and image quality of acquired DWI data. Both goals address the objective to provide a systematic evaluation of the next generation of diffusion modeling tools so that they may be used in the most effective way.

Methods:
The general approach of this study was to apply four different diffusion MRI models using the same input data sets to determine the relationships between metrics and effects of image quality and experimental design across metrics.
Comprehensive ex-vivo DWI data sets were acquired for four mouse brains and one ferret brain at 7T using 3DEPI with isotropic resolution of 100 and 250 um^3 voxel size for mouse and ferret respectively. The full data set contained 297 DWIs with 8-shells of b=100-10,000 s/mm^2.and was manipulated to generate two subsampled "experimental design" datasets with: 5-shells (b=100-1700s/mm^2) and 6-shells (b=100-3800s/mm^2) and three additional "image quality" datasets with: 0%, 5%, 10% and 25% added rectified noise.
Four representative models were applied to the full and manipulated data sets including:
Diffusion Tensor Imaging (DTI[1,2]) with metrics of Trace(D) and fractional anisotropy (FA)
Diffusion kurtosis imaging (DKI[3,4]) with metrics of mean kurtosis (Kmean) and kurtosis FA (KFA)
Mean apparent propagator (MAP[5]) MRI with metrics of return to the origin probability (RTOP), non-Gaussianity (NG) and propagator anisotropy (PA)

Neurite orientation dispersion distribution imaging (NODDI[6]) with metrics of compartmental volume fractions for intracellular restricted (V_{IR}), isotropic free (V_{ISO}) and intracellular (V_{IC}) as well as the orientation dispersion index (ODI)
To evaluate between-metric relationships 2D histogram analysis along with targeted ROI measurements were performed to compare isotropic and compartmental higher order metrics with TR and to compare higher order metrics of anisotropy and dispersion with FA.
The effects of experimental design and noise on each metric were evaluated using within-metric comparisons of whole brain histograms and maps generated by modeling of subsampled and noise-added data sets.

Results:
Comparisons between TR and higher order metrics revealed several notable observations (figures 1 and 2). The Kmean and rtop both demonstrated an inverse relationship with TR showing high sensitivity in regions of low diffusivity. The NG metric appeared to have a more clustered relationship with TR. NODDI compartment fractions were found to have differing relationships with the TR. V_{IR} was close to zero for most gray matter regions and increased primarily in white matter, while V_{IC} showed a range of values across tissue types with a large number of voxels following a negative correlation with TR. While some general trends were evident, no single relationship emerged for compartmental metrics and TR.
Comparisons of higher order metrics of anisotropy and dispersion with FA showed distinct patterns for the whole brain and for regions of white matter with different fiber geometry (figure 3). The KFA appeared directly related to FA in white matter, but clustered in the gray matter. The ODI followed an expected negative relationship with FA according to white matter complexity. The PA remained high for white matter regions across the full range of fiber geometry and FA.
The dependence of the metrics on experimental design varied widely including: systematic bias of the TR and FA, large changes of histogram mode and shape for DKI measures, NG and PA, compartment-specific changes for NODDI measures, remarkable stability for rtop (figure 4).
The dependence of metrics on image quality was similarly variable (figure 5) with the greatest vulnerability found for metrics derived from the non-Gaussian part of the signal (e.g. Kmean, Kfa, NG, PA) and less vulnerability for metrics derived from the full signal (e.g. NODDI measures and rtop) or only the Gaussian part (i.e. DTI measures).

Discussion and Conclusions:
To better understand the information that can be achieved using different methods for analysis of diffusion MRI data we have systematically investigated DTI, DKI, MAP-MRI and NODDI metrics to determine several promising improvements in sensitivity, specificity and novel information. We have also shown that the experimental design and image quality of DWI data sets influence the metrics of these models to different and sometimes very high degree.

References:

1. Basser, P.J., Mattiello, J., LeBihan, D., 1994. Estimation of the effective self-diffusion tensor from the NMR spin echo. J Magn Reson B 103, 247–54.
2. C. Pierpaoli, L. Walker, M. O. Irfanoglu, A. Barnett, P. Basser, L-C. Chang, C. Koay, S. Pajevic, G. Rohde, J. Sarlls, and M. Wu, 2010, *TORTOISE: an integrated software package for processing of diffusion MRI data*, ISMRM 18th annual meeting, Stockholm, Sweden, #1597
3. Jensen, J.H., Helpern, J.A., Ramani, A., Lu, H., Kaczynski, K., 2005. Diffusional kurtosis imaging: the quantification of non-gaussian water diffusion by means of magnetic resonance imaging. Magn Reson Med 53, 1432–40.
4. Tabesh, A., Jensen, J.H., Ardekani, B.A., Helpern, J.A., 2011. Estimation of tensors and tensor-derived measures in diffusional kurtosis imaging. Magn Reson Med 65, 823–36.
5. Özarslan, E., Koay, C.G., Shepherd, T.M., Komlosh, M.E., İrfanoğlu, M.O., Pierpaoli, C., Basser, P.J., 2013. Mean apparent propagator (MAP) MRI: a novel diffusion imaging method for mapping tissue microstructure. Neuroimage 78, 16–32.
6. Zhang, H., Schneider, T., Wheeler-Kingshott, C.A., Alexander, D.C., 2012. NODDI: practical in vivo neurite orientation dispersion and density imaging of the human brain. Neuroimage 61, 1000–16.

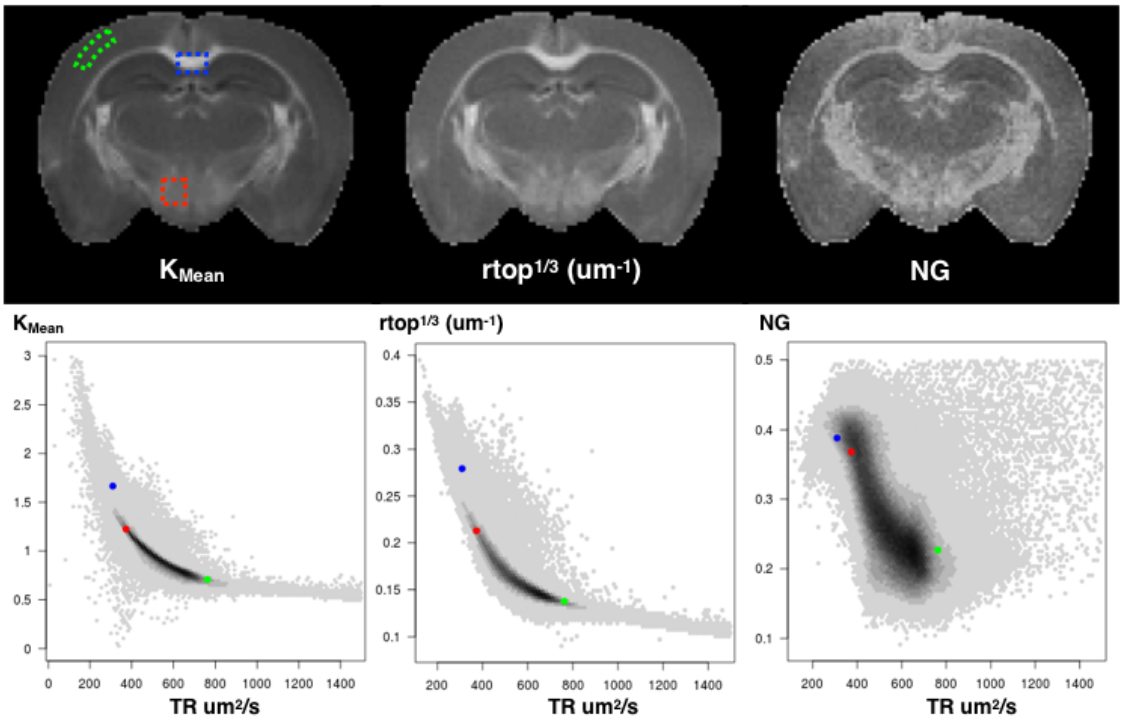

Figure 1. K_{mean}, rtop and NG metric maps are shown with 2D histograms of the whole brain between each metric and TR, where grayscale indicates plot density. Colored ROIs are shown for the cortex (green), corpus callosum (blue) and hypothalamus (red) that correspond to the points plotted against the whole brain histogram.

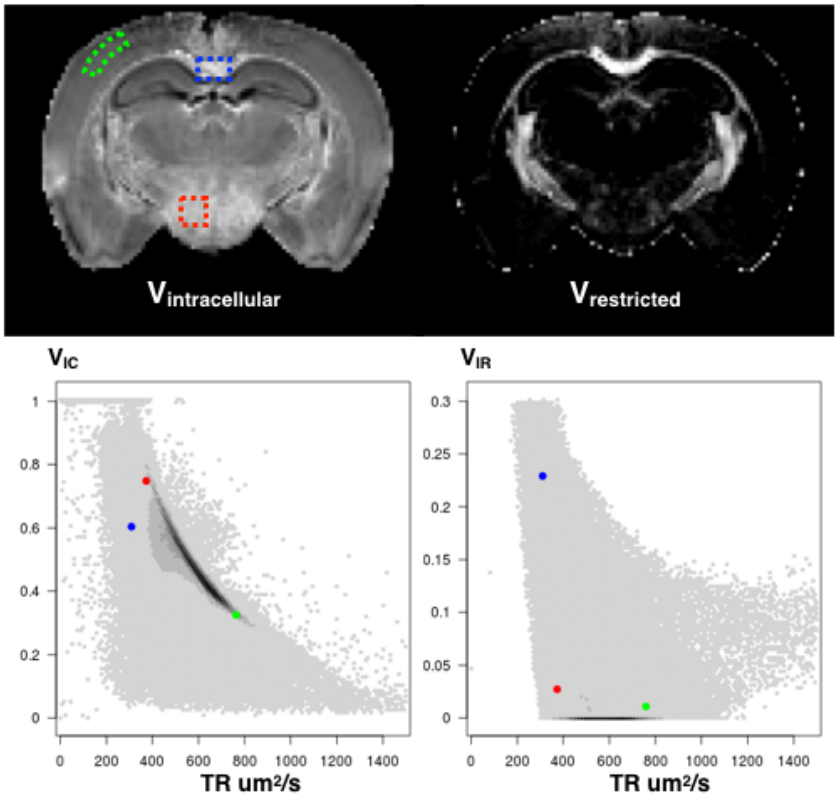

Figure 2. Compartmental volume fraction maps for V_{IC} and V_{IR} are shown with 2D histograms of the whole brain between each metric and TR. Colored ROIs are shown for the cortex (green), corpus callosum (blue) and hypothalamus (red) that correspond to the points plotted against the whole brain histogram.

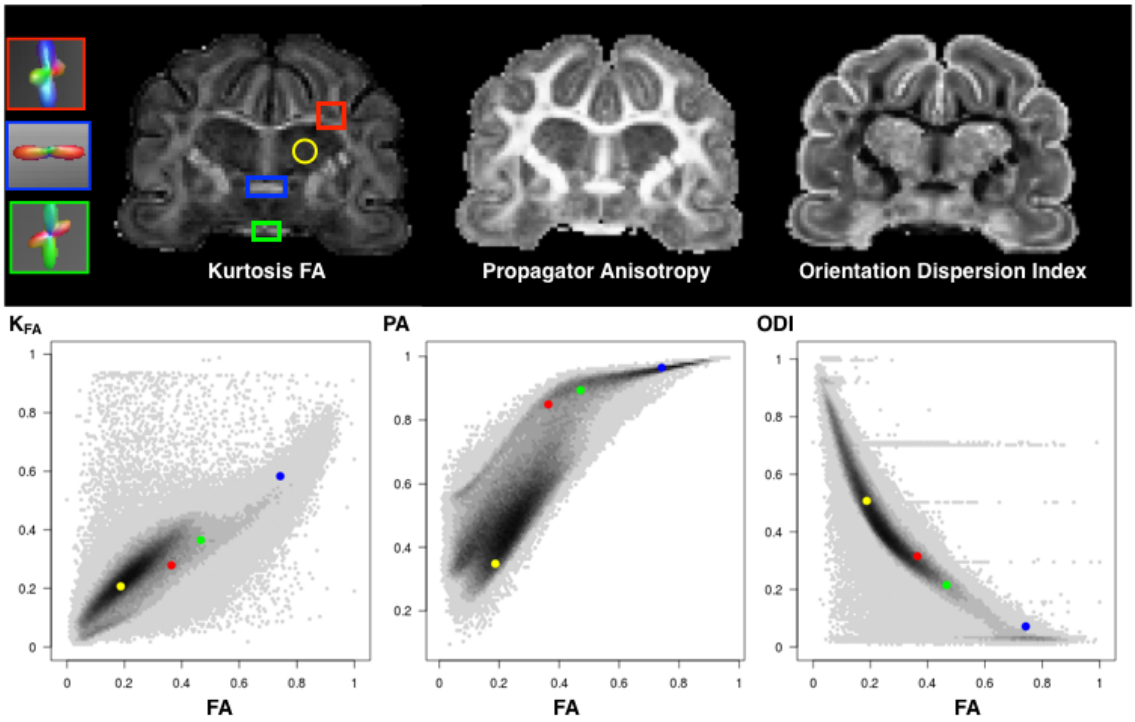

Figure 3. Higher order anisotropy and dispersion metrics, K_{FA}, PA and ODI are mapped in the ferret brain and 2D whole brain histograms are plotted with ROIs for gray matter (yellow) and different fiber geometries: simple (blue), crossing (green) and complex (red).

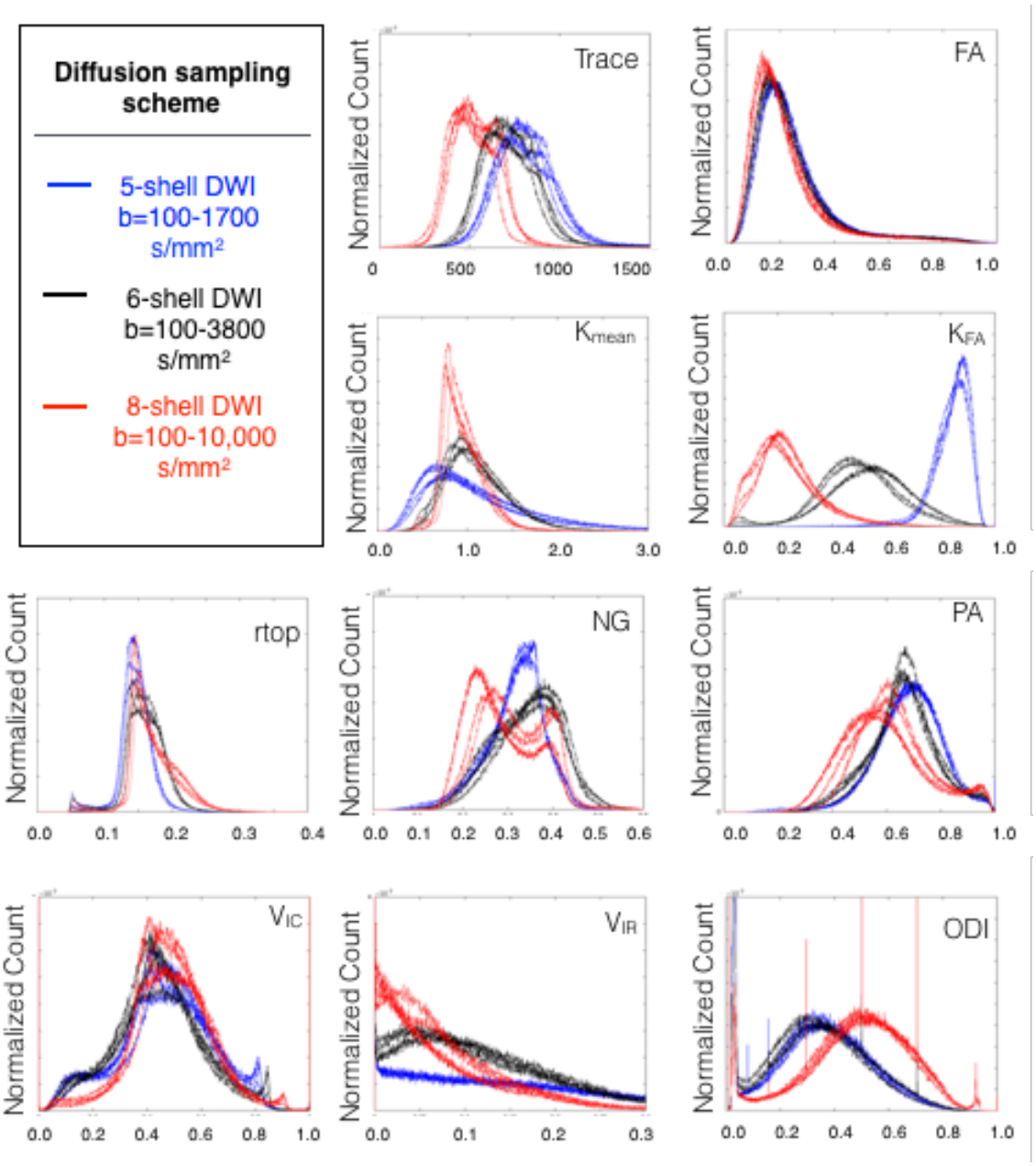

Figure 4. The effects of experimental design are on different metrics are shown by the distribution of metric values in whole brain histograms for 4 mouse brains. The black, blue and red curves were generated from the 5-, 6- and 8- shell data sets respectively.

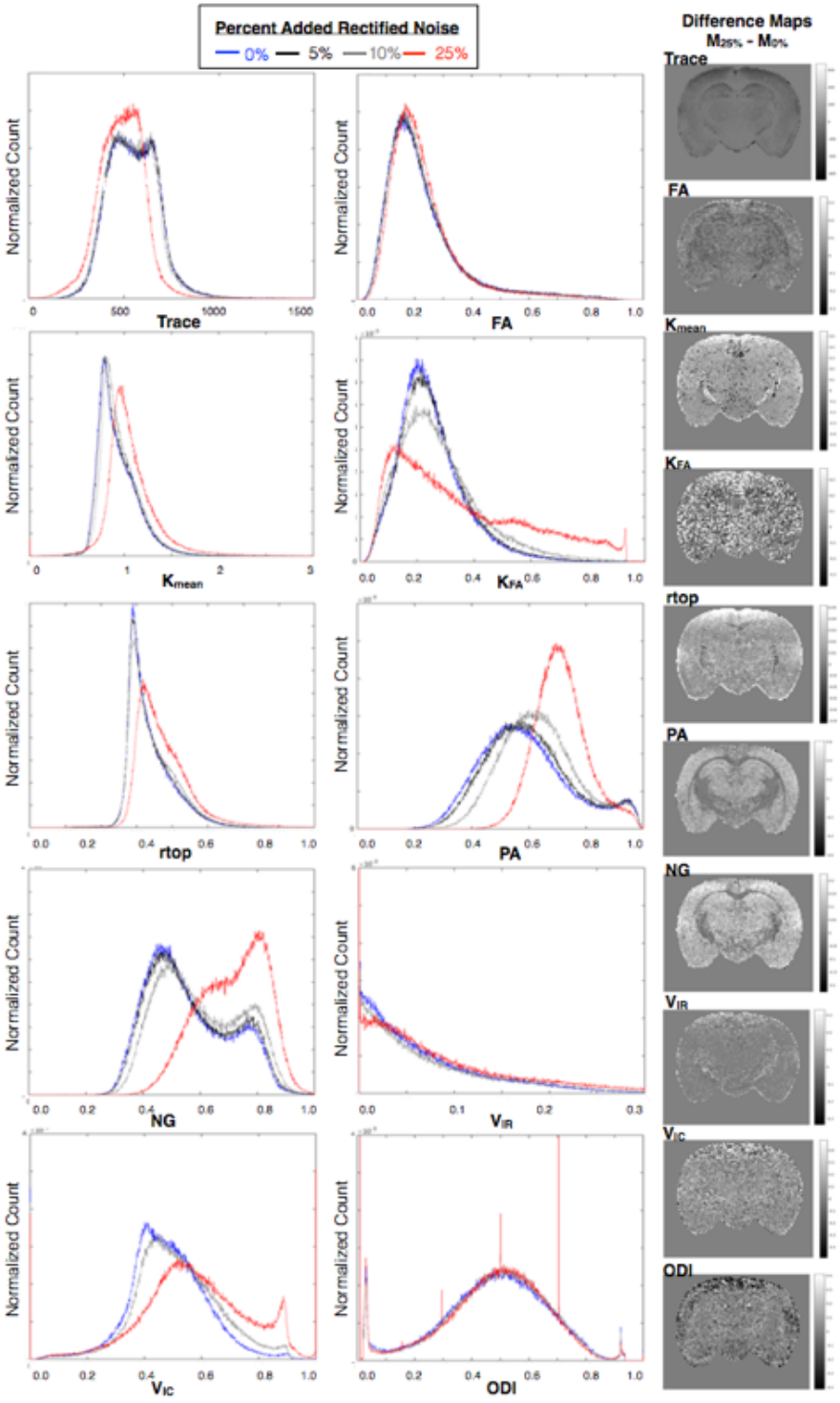

Figure 5. The effects of image quality on different metrics are shown by the distribution of metric values in whole brain histograms for metrics generated from DWIs with different levels of added noise. The blue, black, grey and red curves correspond to 0%, 5%, 10% and 25% added noise.